

THE DYNAMIC BEHAVIOR OF TRANSFORMER CORES

A Thesis

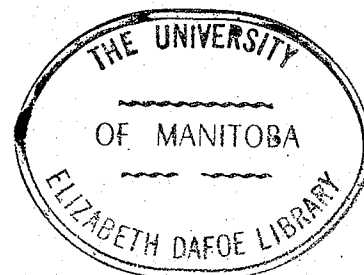
Presented to the Faculty of Graduate Studies and Research
University of Manitoba

In partial fulfillment of the requirements for the degree
MASTER OF SCIENCE IN ELECTRICAL ENGINEERING

by

John Douglas Poustie

May , 1970



ABSTRACT

This investigation was concerned initially with comparing the dynamic, or time varying, behaviour of two very different transformer cores. The various electrical characteristics of a core-winding assembly sometimes used as a "current transformer", and known as a bushing type C.T., were compared with the responses of a modified core and coil assembly taken from a power distribution transformer.

The relevant measurement techniques were thoroughly analyzed and are shown in the Appendix.

It was demonstrated that binomial equations; in one case a quintic, in the other a septic; are a fairly good representation for the average of the flux density vs magnetic field intensity, or B-H, characteristics. For certain situations, the average of the B-H curve may be represented by three segment straight line approximations.

The availability of a reliable two term equation is potentially very useful in harmonic or ferroresonant studies. Recent work has indicated that, for the investigation of the latter, loss representation is not of prime importance to the transformer model.

Using the binomial equations to model the core characteristics, the relationship between applied RMS voltage and resulting RMS current was developed.

A second prime concern of this investigation was the attempt to demonstrate that, for a series circuit containing linear resistance and capacitance as well as non-linear inductance, the analytical prediction of various aspects of ferroresonant behaviour was relatively straightforward.

if the above binomial approximations are used, and that the agreement with test results was quite reasonable. Certain generalizations were made in regard to the "incremental describing function" for an odd powered polynomial relationship between current and flux linkages.

Finally, the excitation of the second and third subharmonics was accomplished and recorded, although no mathematical analysis was attempted in this area.

ACKNOWLEDGEMENT

The author wishes to thank Dr. G. W. Swift for suggesting the topic, arranging financial assistance through the National Research Council of Canada, and for his helpful suggestions during work on this thesis.

In addition, the help obtained from E. A. Dillon of Pioneer Electric Co. to obtain suitable core and coil samples is much appreciated.

John Poustie, B.Sc.(E.E.)

TABLE OF CONTENTS

	PAGE
ABSTRACT	ii
ACKNOWLEDGEMENT	iv
LIST OF ILLUSTRATIONS	viii
INTRODUCTION	xi
 CHAPTER	
I . CONSTRUCTION OF CORE - COIL SAMPLES	I
II. RMS VOLTAGE AND CURRENT CHARACTERISTICS	6
RMS responding meters	6
Comparison of magnetization characteristics	9
Harmonics in the excitation current	9
Relationship of magnetization current to BH curve	16
A physical explanation for magnetization curves	20
III. RMS VOLTAGE VS WATTS CHARACTERISTICS	22
Power measurements : the wattmeter	22
Comments on core loss characteristics	24
Mathematical analysis of core losses	26
Verification of the Steinmetz Exponent	27
Discussion of ferromagnetism and losses	28
IV . FLUX DENSITY VS MAGNETIC FIELD INTENSITY CURVES	33
Presentation of BH characteristics	33
Polynomial relationship between flux linkages and	36
current .	

CHAPTER	CONTENTS	PAGE
	RMS currents resulting from the binomial relationship between current and flux linkages	38
	RMS currents resulting from a segmental relationship between current and flux linkages	46
	Use of the average current / flux linkage equation . . .	51
V .	THE BH CURVE DURING AN INRUSH TRANSIENT	57
	Inrush measurements	57
	Simplified analysis of the most severe condition	59
VI .	SUBHARMONIC RESPONSE OF AN OPEN CIRCUIT TRANSFORMER IN SERIES WITH CAPACITANCE AND RESISTANCE	63
	Second subharmonic	63
	Third subharmonic	66
VII.	FERRORESONANT RESPONSE OF AN OPEN CIRCUIT TRANSFORMER IN SERIES WITH CAPACITANCE AND RESISTANCE	69
	RMS volt - ampere characteristics	69
	Analytical prediction of ferroresonant behavior	72
	i . Reformulation into control system configuration .	74
	ii. The Incremental Describing Function	75
	iii. The stability criterion	82
	iv . The real circuit	83
	Concluding remarks	86

CONTENTS

PAGE

APPENDIX

A . HARMONIC COMPONENT MEASUREMENT 87

B . DETERMINATION OF DYNAMIC BH CURVES USING AN OPERATIONAL
AMPLIFIER TECHNIQUE 90

C . FOURIER ANALYSIS OF POWERS OF THE COMMON TRIGONOMETRIC
FUNCTIONS , IN TABLE FORM 98

D . INVERSION OF THE INCREMENTAL DESCRIBING FUNCTION 100

BIBLIOGRAPHY 103

LIST OF ILLUSTRATIONS

FIGURE		PAGE
I.	Current transformer (CT) details	2
2.	Power transformer (PT) details	2
3.	CT core construction	3
4.	PT core construction	3
5.	The circuit used to measure magnetization characteristics . .	7
6.	Showing possible distortion of V_t and I_s	7
7.	a) Magnetization characteristics (CT and PT)	IO
	b) Volt - amps per pound vs. flux density (CT and PT)	II
8.	Tracings of voltage and current waveforms for the CT and PT , under open circuit conditions	I2
9.	a) PT harmonic analysis (test results)	I3
	b) CT harmonic analysis (test results)	I4
IO.	Typical BH curve	I7
II.	Current resulting when saturation only is represented	I7
I2.	Current resulting when saturation and hysteresis are both . . represented	I8
I3.	Current resulting when all losses are considered	I9
I4.	BH curves for different voltages	2I
I5.	Circuit used for power measurement	23
I6.	Details of the electrodynamicometer movement	23
I7.	Core loss data	25
I8.	Tracing of the CT BH curves	29
I9.	Tracing of the CT BH curve photos , for a fixed flux density , and a range of frequencies	29
20.	Plot of relative loss per cycle vs. frequency (CT and PT) .	30
2I.	BH curve photo tracings (CT)	34
22.	BH curve photo tracings (PT)	35

ILLUSTRATIONS

FIGURE	PAGE
23. The curve of interest	37
24. Current / flux linkage relationships for the PT	39
25. Current / flux linkage relationships for the CT	40
26. Comparing calculations and test results (PT)	43
27. Comparing calculations and test results (CT)	45
28. Symbols and waveforms	47
29. a) Calculated magnetizing amps for the CT	52
b) Harmonics in the CT excitation current , comparing calculations and test data	53
30. a) Calculated magnetizing amps for the PT	54
b) Harmonics in the PT excitation current , comparing calculations and test data	55
31. CT inrush transients	58
32. PT inrush transients	60
33. Simplified inrush analysis	61
34. The circuit of interest	64
35. Inductor voltage while the second subharmonic existed	64
36. Circuit current , showing the second subharmonic	65
37. Mains voltage and current	65
38. BH curve when the subharmonic exists	67
39. BH curve when the third subharmonic exists	67
40. The CT voltage	67
41. Volt - ampere characteristics	70
42. The circuit of interest.	73
43. Reformulation into control system form	76
44. Determination of the critical voltage	85

ILLUSTRATIONS

FIGURE		PAGE
A.I	Circuit for determining harmonic components of the transformer exciting current	88
B.I	Circuitry necessary to display the BH curves of a transformer	91
B.2	Modified operational amplifier network , showing the integrator and the LF rejection network	93
B.3	Equivalent circuit for an unmodified operational integrator	93
B.4	Steps in the evaluation of the transfer function	95
B.5	Further steps in the evaluation of the transfer function	95
B.6	Frequency response curves for the modified , and the unmodified integrator networks	97
D.I	Locus of K_e in the 'Z' plane	IOI
D.2	Locus of the inversion of K_e in the 'W' plane , where $W = I / Z$	IOI

INTRODUCTION

The first real objective of this thesis, which is an offshoot of the Doctoral Dissertation presented to Illinois Institute of Technology by G. W. Swift, was to obtain accurate flux density vs magnetic field intensity curves. These curves, also called B-H curves, were obtained by operational simplifier techniques and allow several electrical characteristics to be deduced regarding the sample, if frequency, flux density and time of switching are the experimental variables. Of most interest was the binomial equation, $i = C_1 \ell + C_n \ell^n$ which was proposed as the arithmetic average of the ℓ/i relationship, which is directly proportional to the B/H relationship.

In the previously mentioned Ph.D. thesis, the equation:

$$i = \ell + 4\ell^5$$

was presented as the per unit binomial best fitting the core and coils of a 5 kva distribution transformer manufactured by the Commonwealth Edison Co. of Chicago. Although the details of the core's construction were not known to the present author, it was of interest to compare the same results to the two cores of this thesis, for which constructional details were known.

It was also of interest to derive the theoretical "magnetization curve", that is, the I(RMS) vs E(RMS) relationship, using the binomial i/ℓ equation as the starting point, and then to compare the results with the actual magnetization test on the same core. Since agreement was not too close, presumably due to the inadequate modelling of iron losses, no

attempt was made to obtain the i/ℓ curve from the actual magnetization test results. The latter procedure would have been very useful, since to date, transformer manufacturers are not obliged to furnish B-H curves, but normally provide the magnetization data obtained from the acceptance tests.

While examining the ferroresonant response of a series R-L-C circuit, the author was able to measure the second and third subharmonics, and also became interested in the methods available for predicting ferroresonance analytically, and Chapter Seven represents an attempt to reconcile a mathematical prediction based on an approximate model to the measurements made on the circuit in the laboratory situation.

CHAPTER I

CONSTRUCTION OF CORE-COIL SAMPLES

The object of this Chapter is to compare physically the available test samples. The abbreviations C.T. and P.T. shall be used for "current transformers" and "power transformers" respectively.

Figure 1 gives physical details of the C.T. core, while in Figure 2, the P.T. is detailed.

Since the cores were available initially without windings, it was necessary to determine the number of turns to wind in order to accomplish further testing. In general, this is determined by applying the equation

$$E = \frac{4.44 fN (B_m A_n)}{10^8}$$

where E = RMS voltage [usually called "rated" voltage],

f = frequency

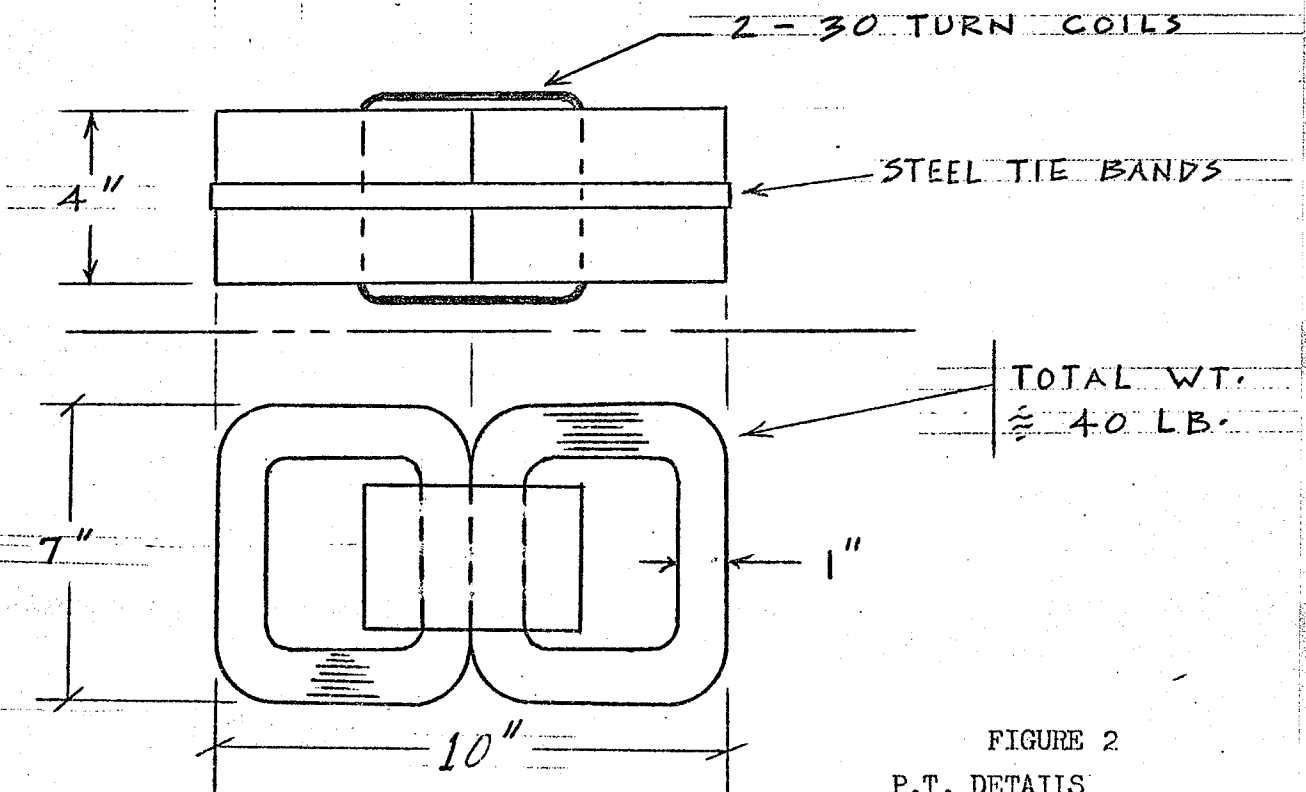
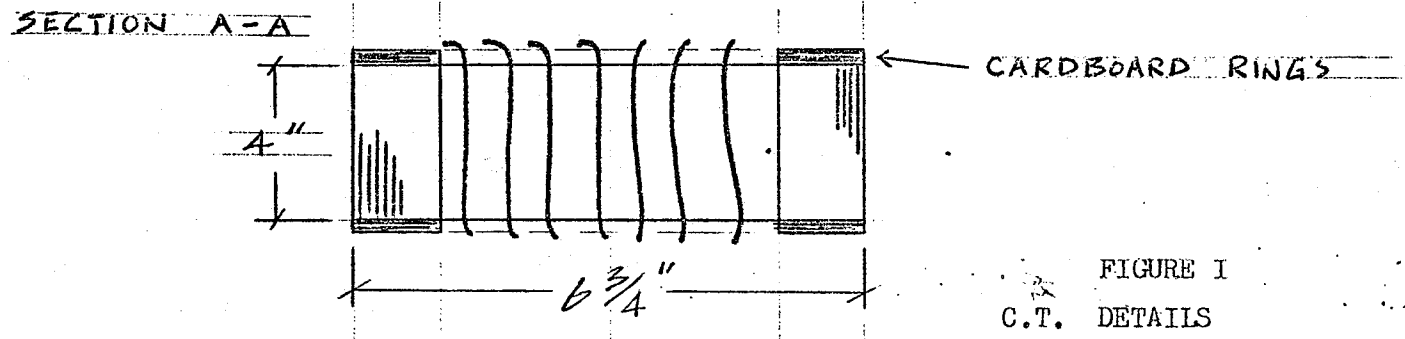
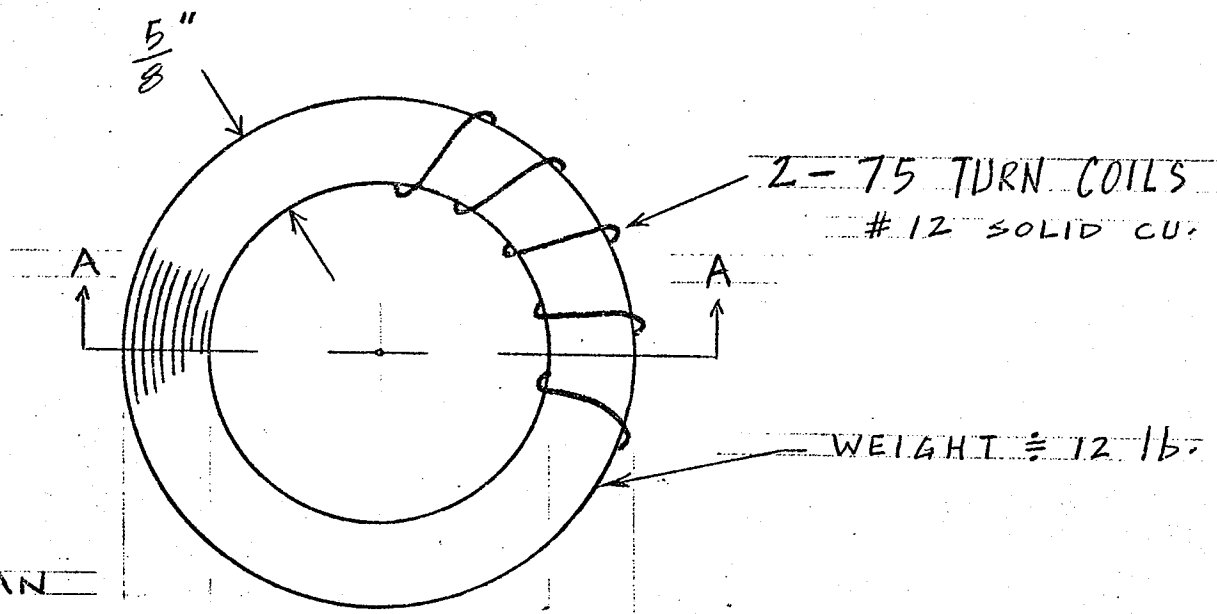
N = number of turns (to be found)

B_m = peak flux density (to be chosen)

A_n = net steel cross sectional area.

If E is chosen, and since in this instance A_n is fixed, B_m is then chosen to restrict exciting current, as well as total core loss. Depending on steel type and treatment, and core construction, B_m may vary over a wide range.

For the C.T., E was chosen for convenience in testing to be 50 v RMS, and a figure of $B_m = 100$ kilolines/in² was thought to be



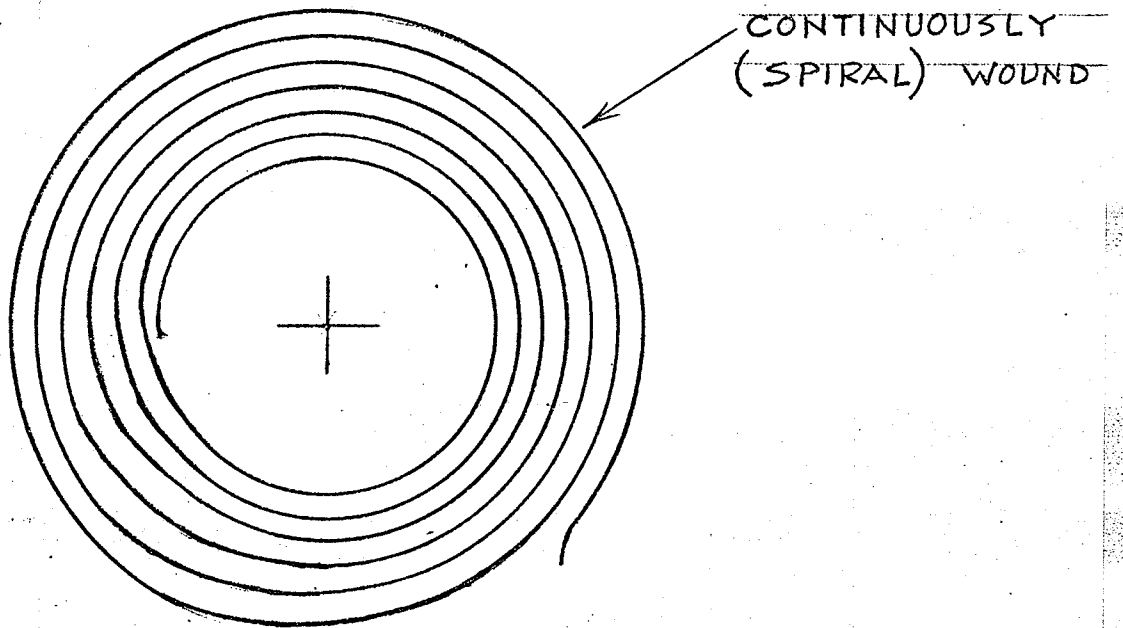


FIGURE 3
CT CORE CONSTRUCTION

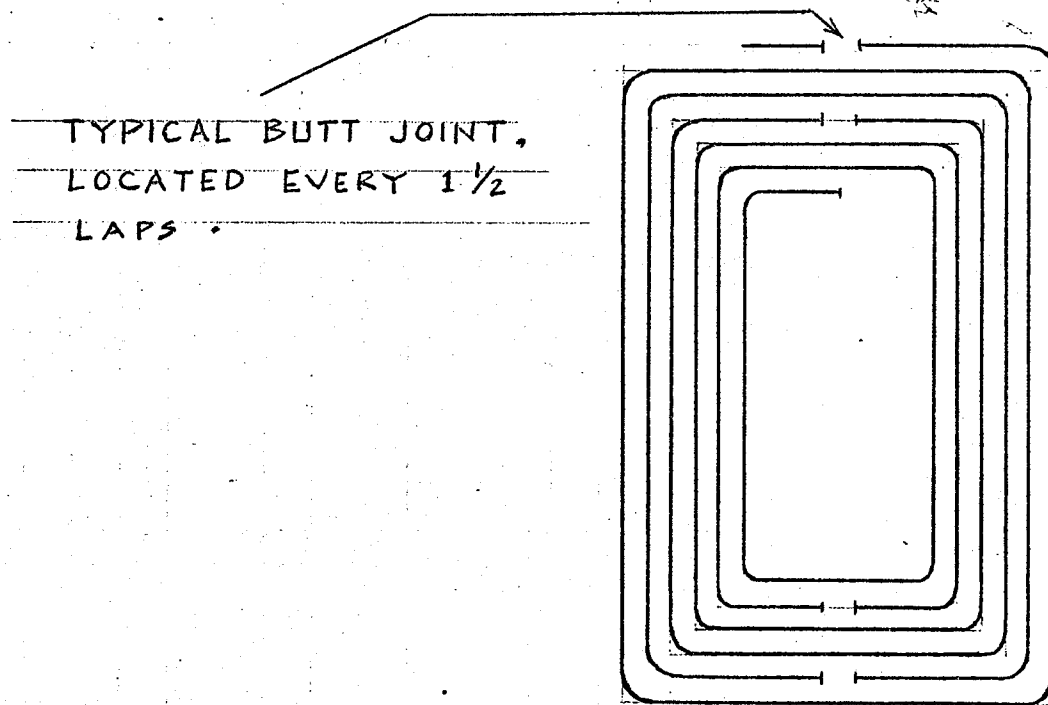


FIGURE 4
PT CORE CONSTRUCTION

satisfactory. This determined $N = 75$ turns. Two identical windings, of 75 turns and using #12 Heavy Formel solid copper were wound to allow the measurement of B-H curves, using an operational amplifier technique which will be explained later. The wire gauge was heavy enough to prevent winding overheating under all anticipated test conditions.

In the case of the P.T., E was also chosen to be 50 v RMS, while $B_m = 83$ kilolines/in² was used to restrict excitation current. Available test data on cores of similar construction indicated that excitation current would be much higher for the P.T. than for the C.T. core. Calculations indicated that 30 turns should be satisfactory, and two identical, 30 turn, #12 HF copper windings were wound as shown in Figure 2.

The material used in both cores was a modern, grain oriented transformer steel of approximately 11 mils thickness. The objective at this point was to emphasize differences in core cutting and assembly, rather than to discuss manufacturing specifications for the steel. To this end, Figures 3 and 4 illustrate core construction. It was felt that these samples represented extreme cases. The C.T. core could be said to approach the ideal, that is, fairly tightly wound on a machine, employing high grade steel, with no air gaps in the magnetic circuit, and no small radius bends in the steel. The P.T., on the other hand, which in this instance was salvaged, had air gaps (which tended to cause flux concentration) at 4 points on its periphery. It was assembled by hand onto the coil, and could have been mishandled, thus causing increased eddy current losses where interlayer insulation was scraped off, in addition to introducing metallic stresses which could not be relieved by "soaking" in a high temperature oven after the coil had been assembled on the core.

It is held by the author that the core of a large power transformer would lie in between the P.T. and the C.T. as far as the number and size of air gaps in the core, and relative amount of human handling goes.

This fact, then, might permit the application to large power transformers of some of the conclusions drawn in this thesis.

The author makes the presumption here of some prior knowledge of power transformer core assembly by his examiners.

CHAPTER II

RMS VOLTAGE AND CURRENT CHARACTERISTICS

The object of this Chapter is, at the same time as presenting comparative measurements of magnetization or open circuit data, including harmonic component determination, to examine the techniques used to obtain these characteristics.

Also, an attempt is made employing graphical analysis to show the influence of the shape of the B-H curve on the excitation current waveform.

Finally, an explanation for the shape of the actual magnetization curve is attempted, based on the B-H curve measurements to be presented in future chapters.

2.1 RMS responding meters.

Proper measurement of power frequency voltage and current was complicated by the following. While many types of meters, including Volt-Ohm Meters, Vacuum Tube Voltmeters, and moving iron instruments will read perfectly sinusoidal voltages accurately (assuming proper calibration), the source impedance may, in some instances, be sufficiently high to cause the terminal voltage to be distorted, especially when currents flowing to the transformer on open circuit are not perfectly sinusoidal. Figure 5 depicts this circuit in a very general way, while Figure 6 shows what type of distortion could occur in the terminal voltage for an assumed current waveform. For an inductive source impedance, the harmonic distortion is intensified, since the current, the waveform of which is said to contain "harmonics", or higher frequency components, causes a relatively

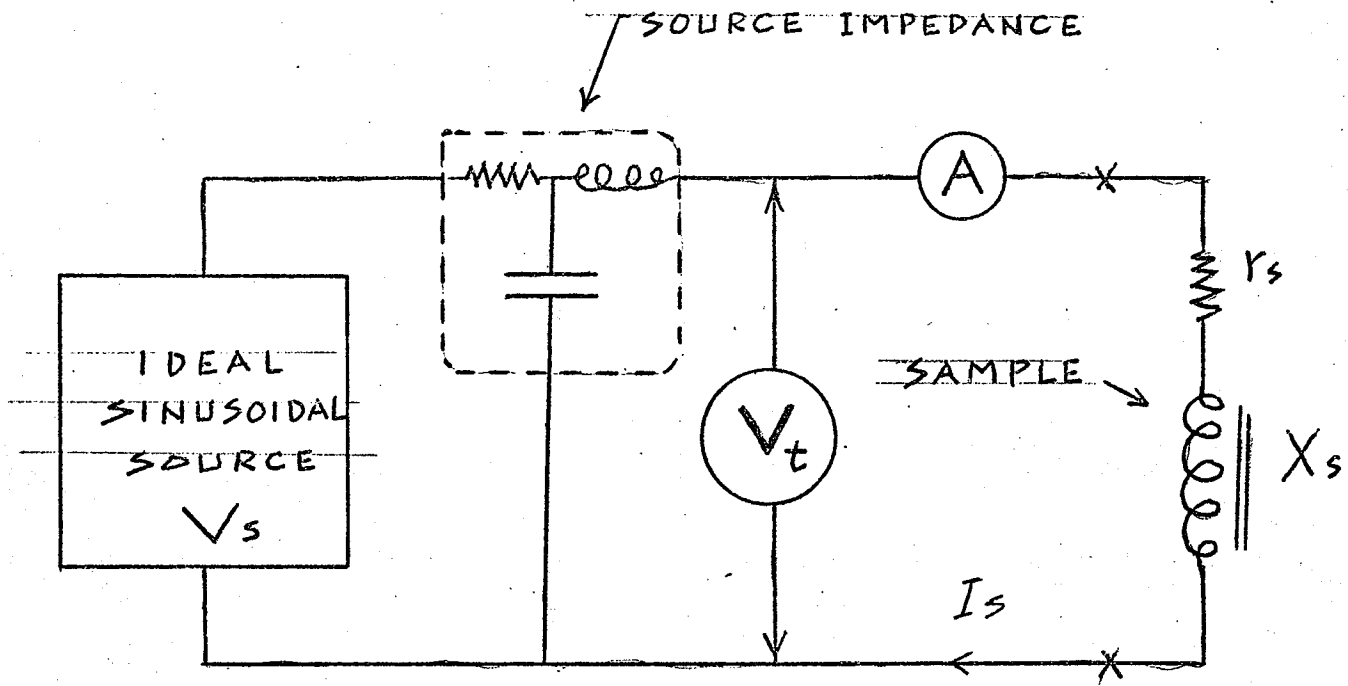


FIGURE 5
THE CIRCUIT USED TO MEASURE MAGNETIZATION CHARACTERISTICS

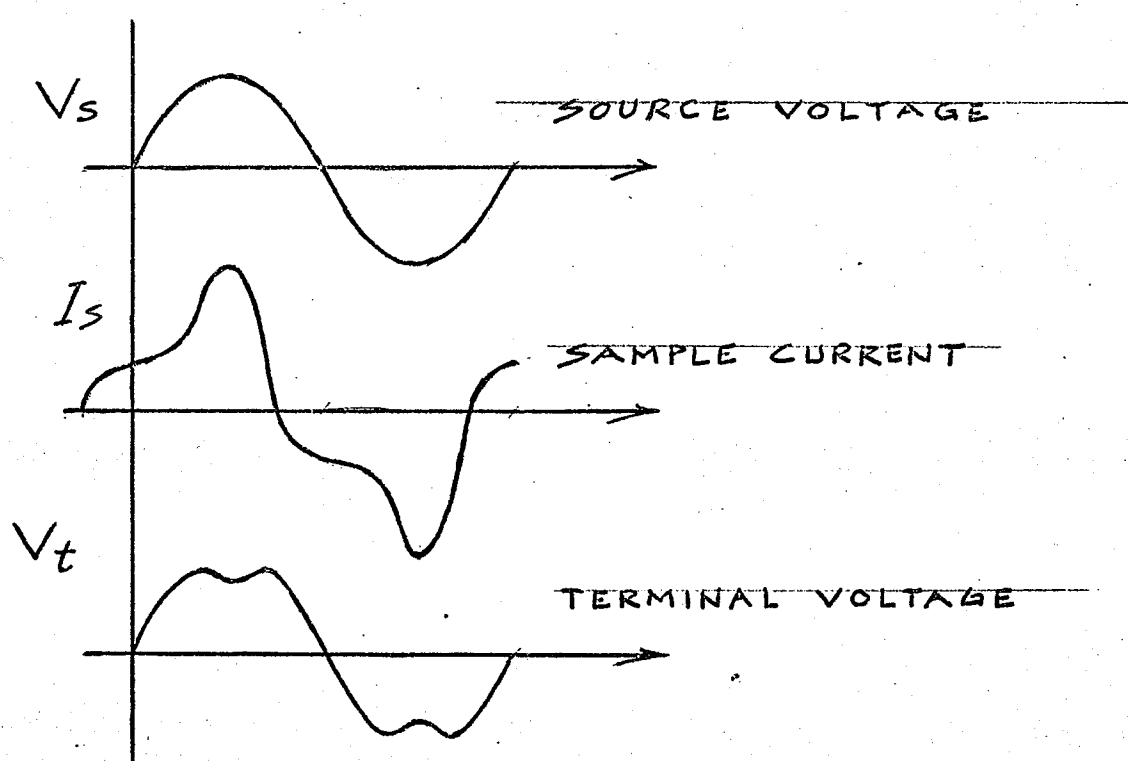


FIGURE 6
SHOWING POSSIBLE DISTORTION OF V_t & I_s

larger harmonic voltage drop across this same inductive source reactance. In transformer test installations, tooth ripple in the supply generator might cause unwanted (higher frequency) peaks in the test voltage.

It must be remembered that a VTVM, depending on the manufacturer, might respond either to the 0-peak or the peak-peak of a rectified sine wave. It is to be stressed that the VTVM is calibrated on a sinusoidal waveshape and will be in error for any distortion in the measured voltage. Similarly, a VOM will respond accurately to a sinusoidal voltage only; its movement being of the d'Arsonval type, fed from either a full wave or half wave rectifier unit.

In a meter having the moving iron type of construction, angular deflection is proportional to the square of the operating current and the rate of change of inductance with respect to angular deflection, so that calibration may be accomplished in terms of effective [RMS] voltage or current. According to Harris, "The waveform error of a modern instrument with short vanes is negligible for the third harmonic at power frequencies".

During the magnetization current measurements associated with this thesis, the author checked the applied voltage waveform with an oscilloscope to ensure that no distortion occurred. In this instance, the currents encountered were not larger than 3% of the source RMS current rating. Voltage magnitude was measured with a 75 volt range moving iron meter, while RMS currents were determined with a moving iron meter rated 1 amp RMS.

In a situation where source voltage distortion exists, the conversion of results back to an equivalent sine wave basis is exceedingly complicated. The interested reader is referred to Chapter II of reference # 3 in the bibliography.

2.2 Comparison of Magnetization Characteristics.

The characteristics are presented in Figure 7 A and 7 B . Certain similarities between the curves of 7 A deserve comments. Current increased with voltage, but not in a linear fashion, even for lower values of voltage. In both cases, as expected, $\Delta I/\Delta V$ becomes very large for larger voltages. On the other hand, the basic curve shapes are dissimilar, that is, the curves could not be superimposed in a per unit sense, even if different base quantities were chosen.

A transformer designer might point out that 83 kilolines per square inch was a poor choice for the design figure for the P.T., since the magnetization curve indicates that the core is into the saturation region at 50 volts RMS applied. The curve shows that 30 to 35 volts would have been a better choice for the "rating", now that the core is assembled. The C.T. design, however, worked out quite well for the assumptions made.

In Figure 8, tracings of the photographs of the actual current waveforms are shown. The large amount of distortion present in the C.T. current waveform is contrasted to the P.T. waveform at the chosen "rated" voltages.

It is to be stressed that the P.T. has, overall, a much more linear magnetization characteristic than does the C.T.

2.3 Harmonics in the Excitation Current.

It is of interest to analyze the excitation current waveform for both the C.T. and the P.T. The measurement technique used to accomplish this is analyzed in Appendix A. The results of these measurements are shown in Figure 9. The following calculations demonstrate the